





Uniaxial modulation and the Berezinskii-Kosterlitz-Thouless transition

Domenico Giuliano ^{1,2} Phong H. Nguyen ^{3,4} Andrea Nava ^{1,2,5} and Massimo Boninsegni ³

¹*Dipartimento di Fisica, Università della Calabria, Arcavacata di Rende, I-87036 Cosenza, Italy*

²*I.N.F.N., Gruppo Collegato di Cosenza, Arcavacata di Rende, I-87036 Cosenza, Italy*

³*Department of Physics, University of Alberta, Edmonton, Alberta, Canada T6G 2E1*

⁴*Faculty of Physics, VNU University of Science, Vietnam National University, 334 Nguyen Trai Street, Thanh Xuan, Hanoi, Vietnam*

⁵*Institut für Theoretische Physik, Heinrich-Heine-Universität, D-40225 Düsseldorf, Germany*



(Received 23 February 2023; revised 14 May 2023; accepted 19 May 2023; published 30 May 2023)

We present a theoretical study of the Berezinskii-Kosterlitz-Thouless transition of a two-dimensional superfluid in the presence of an externally imposed density modulation along a single axis. The subject is investigated in the context of the $|\psi|^4$ classical field theory, by means of analytical and numerical techniques. We show that, as the amplitude of the modulation increases, the physics of the system approaches that of the anisotropic x - y model, with a suppressed superfluid transition temperature and an anisotropic response, but with no dimensional crossover.

DOI: [10.1103/PhysRevB.107.195439](https://doi.org/10.1103/PhysRevB.107.195439)

I. INTRODUCTION

The intriguing behavior of a quantum fluid in reduced dimensions continues to elicit considerable research activity, in part motivated by recent experimental advances, allowing one to investigate, e.g., superfluid helium films or cold-atom assemblies in novel, yet unexplored settings.

The superfluid transition of a Bose fluid in three dimensions (3D) occurs at the critical temperature T_c , concomitantly with the onset of Bose-Einstein condensation, namely, the appearance of off-diagonal long-range order (ODLRO) [1,2]. By contrast, in two dimensions (2D) the superfluid phase displays no true ODLRO at any finite temperature, but rather a slow (power-law) decay of spatial correlations. The superfluid transition in 2D is theoretically understood within the Berezinskii-Kosterlitz-Thouless (BKT) general framework [3–5]; the characteristic fingerprint of the BKT transition is the so-called “universal jump” of the superfluid fraction $\rho_s(T)$ as a function of temperature, from zero to a finite value as T_c is approached from above [6–9].

Yet another paradigm change takes place if the system is confined to just one dimension (1D), for in that case a comprehensive description of its low-lying excitations and its ensuing thermodynamic properties is provided by the Tomonaga-Luttinger liquid theory [10]. While, strictly speaking, no superfluid phase exists in 1D in the thermodynamic limit (i.e., $L \rightarrow \infty$, L being the system size), one can still meaningfully speak of “superfluidity” of a 1D system as a well-understood and characterized finite-size effect, i.e., $\rho_s(L, T)$ is a universal function of LT [10–12]. It should also be noted that, although no superfluid (i.e., indefinitely long-lived) current can in principle be sustained in 1D, nonetheless the physical mechanism that leads to current decay in 1D, namely, phase slips [13–17], can be strongly suppressed at low temperature, to the point where there may be no practical experimental difference between a current-

carrying state in 1D and a 3D superfluid [18]. Moreover, there exist theoretical scenarios in which 3D superflow could be established in a network of interconnected quasi-1D channels [19,20].

Experimental verification of the BKT transition has been achieved in a variety of physical settings, including superfluid (^4He) [21–26] and superconducting [27] thin films, Josephson junction arrays [28], and, relatively more recently, cold-atom assemblies [29–32]. In order to observe Luttinger liquid behavior, several experimental avenues have been considered to confine quantum fluids such as ^4He in (quasi) 1D. In particular, the adsorption of helium gas inside elongated cavities of nanometer-size diameter, such as those that exist in a variety of porous glasses [33–38], or nanoholes in Si_3N_4 membranes [39], as well as carbon nanostructures [40,41], has been vigorously pursued, seen as it was as the most promising approach. More recently, however, interesting alternatives have emerged, such as self-assembled chains of atoms on surfaces [42] and cold atoms [43–45].

The remarkable degree of control that has been attained on many of the relevant systems that have been investigated allows one to pose fundamental theoretical questions on the physics of superfluids in reduced dimensions, making predictions for which actual experimental verification may be feasible. One such question is whether it is possible, by tweaking an external parameter, to change the effective dimensionality of a superfluid and observe the ensuing change in the behavior of the system, described by the abovementioned, different theoretical frameworks [46]. Some of these issues have already been explored in the context of dipolar assemblies of cold atoms or molecules, which can form 3D parallel stripes (elongated droplets in finite systems) [47,48] whose collective behavior can mimic that of a 2D cluster crystal [49,50].

But even if interactions among the constituent particles are isotropic, one can imagine inducing a dimensional crossover

by superimposing, e.g., to a quasi-2D Bose gas, an external modulating potential of variable amplitude *along a specific direction*. In this setup, which is well within the reach of current experimental cold-atom technology [43,51,52], one should observe the breakdown of the system into nearly independent, quasi-1D stripes (or “tubes”), for sufficiently large amplitude of the external potential, conceivably accompanied by a change in the physical behavior of the system, reflecting an effective change of dimensionality, from 2D to 1D. This behavior would allow, for instance, by means of pertinent modulating potentials, to mimic quasi 1D systems with nontrivial topology such as, for instance, junctions and/or networks of 1D channels [53–57] or to realize in a tunable and controlled way the physics associated to the topological Kondo effect [58–64].

With the aim of characterizing such a possible dimensional crossover, we investigate this scenario theoretically within the framework of the classical $|\psi|^4$ lattice field theory. The reason for this choice is that, despite the obviously oversimplified description that this model provides of the system of interest, it nonetheless features all the physical aspects that we wish to explore; i.e., it displays a BKT superfluid transition while allowing for an externally induced density modulation, expressed through the use of a locally varying chemical potential. It also lends itself to a semianalytical analysis, which we then validate quantitatively by means of large-scale, numerical simulations.

Our main finding is that the uniaxial external modulation induces *no* dimensional crossover for any finite value of the amplitude of the modulation. Rather, as the system progressively forms quasi-1D parallel stripes in the direction perpendicular to that of the modulation, its physical behavior approaches that of the classical anisotropic x - y model, i.e., with different coupling along the two directions. In particular, increasing the amplitude of the modulation has the effect of suppressing the superfluid transition temperature T_c , while the anisotropy of the superfluid response can be interpreted as a change of length scale in one of the two directions.

The remainder of this paper is organized as follows: in Sec. II we introduce the model and discuss the main issue of interest, as well as the different investigative methodologies adopted in this work. In Sec. III, we show that model (1) becomes effectively equivalent to an anisotropic x - y model in the limit of large modulation amplitude, and we obtain analytical predictions concerning the superfluid transition. In Sec. IV we assess our analytical predictions against the results of our numerical (Monte Carlo) simulations. We offer our discussion and conclusions in Sec. V, while in the Appendix we provide the mathematical details of the mapping between the $|\psi|^4$ model and the anisotropic x - y model.

II. MODEL

The classical $|\psi|^4$ field theory is defined by the following Hamiltonian:

$$H = -t \sum_{\langle \mathbf{r}\mathbf{r}' \rangle} (\psi_{\mathbf{r}} \psi_{\mathbf{r}'}^* + \psi_{\mathbf{r}'}^* \psi_{\mathbf{r}}) + \sum_{\mathbf{r}} \left(\frac{U}{2} n_{\mathbf{r}}^2 - \mu_{\mathbf{r}} n_{\mathbf{r}} \right). \quad (1)$$

We assume a square lattice of $L \times L$ sites (L even), with periodic boundary conditions in both directions; the position

of a generic lattice site is $\mathbf{r} \equiv (l_x, l_y)$, with l_x and l_y being integers, $1 \leq l_{x(y)} \leq L$. The (first) second sum runs over all (pairs of nearest-neighboring) sites, $\psi_{\mathbf{r}}$ is a complex-valued field defined at site \mathbf{r} , and $n_{\mathbf{r}} = |\psi_{\mathbf{r}}|^2$ is the corresponding density of particles. The parameter t is a particle-hopping energy, which we take as our energy unit and set equal to 1. U (assumed positive in this work) is the characteristic energy of interaction of particles occupying the same site, while $\mu_{\mathbf{r}}$ is a (site-dependent) chemical potential, which we assume to be of the following form:

$$\mu_{\mathbf{r}} = V_0 + V_1 \cos\left(\frac{2\pi m l_y}{L}\right). \quad (2)$$

$\mu_{\mathbf{r}}$ accounts for an external potential, which is taken to be along the y direction and has amplitude V_1 . m is an integer number ranging from 1 to L and commensurate with L , so that the modulation takes place over a period of $N = L/m$.

Equation (1) is the classical limit of the well-known Bose-Hubbard model, approached when the average occupation number $\langle n_{\mathbf{r}} \rangle \gg 1$. In the absence of an external potential (i.e., with $V_1 = 0$), and with $V_0 = U$, Eq. (1) reduces to the well-known x - y model, in the strong coupling (i.e., $U \rightarrow \infty$) limit. In 2D, model (1) displays a BKT superfluid transition, the role of the superfluid response being played by the classical helicity modulus [65]. It constitutes a suitable *minimal* model to gain insight into the physics of interest here, since we aim at determining whether a change in the effective dimensionality of the system occurs for a finite value of the modulation amplitude. Such a change ought to be mirrored in the critical properties of the system, which in turn reflect its behavior over long distances, largely insensitive on whether the underlying field theory is formulated in the continuum or on a lattice or whether it is quantum or classical in character.

It is worth mentioning that the effect of an anisotropic hopping parameter, including the case of spatial modulation in one direction, has been studied in the context of the Bose-Hubbard model [66]. In the model considered in this work, on the other hand, the anisotropy of the physical behavior, including a possible dimensional crossover, arises exclusively from the imposition of an external potential. The advantage of utilizing Eq. (1) as a starting point is that it allows one to establish some basic physical conclusions analytically and test them reliably by means of large-scale numerical (Monte Carlo) simulations.

III. ANISOTROPIC x - y MODEL DESCRIPTION OF THE CLASSICAL $|\psi|^4$ THEORY

Model (1) can be shown to be effectively equivalent to an anisotropic x - y model. We begin by re-expressing the $|\psi|^4$ Hamiltonian using the “polar coordinate” representation for $\psi_{\mathbf{r}}$ given by $\psi_{\mathbf{r}} = \sqrt{n_{\mathbf{r}}} e^{i\theta_{\mathbf{r}}}$, i.e.,

$$H = - \sum_{\langle \mathbf{r}\mathbf{r}' \rangle} t \sqrt{n_{\mathbf{r}} n_{\mathbf{r}'}} \cos(\theta_{\mathbf{r}} - \theta_{\mathbf{r}'}) + \sum_{\mathbf{r}} \left(\frac{U}{2} n_{\mathbf{r}}^2 - \mu_{\mathbf{r}} n_{\mathbf{r}} \right). \quad (3)$$

For U large and $V_0 = U$ one may rely on a saddle-point approximation of the right-hand side of Eq. (3). To do so, one

sets $n_{\mathbf{r}} = \bar{n}_{\mathbf{r}} + \delta n_{\mathbf{r}}$, with $\bar{n}_{\mathbf{r}}$ being the saddle-point solution for $n_{\mathbf{r}}$. Moreover, fluctuations in the phase differences $\theta_{\mathbf{r}} - \theta_{\mathbf{r}'}$ are typically assumed to be of order $(\delta n_{\mathbf{r}})^2$ [67]. Taking that into account, we conclude that $\cos(\theta_{\mathbf{r}} - \theta_{\mathbf{r}'}) \approx 1 + O((\delta n_{\mathbf{r}})^2)$. Therefore, neglecting the coupling between $\delta n_{\mathbf{r}}$ and the fluctuations of $\theta_{\mathbf{r}}$ up to second-order in the fluctuations, we obtain

$$-\sum_{(\mathbf{r}\mathbf{r}')} t\sqrt{\bar{n}_{\mathbf{r}}\bar{n}_{\mathbf{r}'}} \cos(\theta_{\mathbf{r}} - \theta_{\mathbf{r}'}) \approx -\sum_{(\mathbf{r}\mathbf{r}')} t\sqrt{\bar{n}_{\mathbf{r}}\bar{n}_{\mathbf{r}'}} + \sum_{(\mathbf{r}\mathbf{r}')} t\sqrt{\bar{n}_{\mathbf{r}}\bar{n}_{\mathbf{r}'}} [1 - \cos(\theta_{\mathbf{r}} - \theta_{\mathbf{r}'})]. \quad (4)$$

Inserting Eq. (4) into Eq. (3) and equating to 0 the term that is linear in $\delta n_{\mathbf{r}}$, we recover the saddle-point equations for $\bar{n}_{\mathbf{r}}$. These are given by

$$t\{\sqrt{\bar{n}_{(l_x+1, l_y)}} + \sqrt{\bar{n}_{(l_x-1, l_y)}} + \sqrt{\bar{n}_{(l_x, l_y+1)}} + \sqrt{\bar{n}_{(l_x, l_y-1)}}\} = \sqrt{\bar{n}_{(l_x, l_y)}} \{U\bar{n}_{(l_x, l_y)} - \mu_{(l_x, l_y)}\}, \quad (5)$$

with the additional constraint that $\forall \mathbf{r}$ one has $\bar{n}_{\mathbf{r}} \geq 0$. When $t = 0$, Eq. (5) reduces to the ‘‘local density approximation’’ solution, $\bar{n}_{(l_x, l_y)} = \mu_{(l_x, l_y)}/U$ if $\mu_{(l_x, l_y)} > 0$ and $=0$ otherwise. A finite t , instead, implies a finite $\bar{n}_{(l_x, l_y)}$ over each lattice site, even for $|V_1| > |V_0|$.

The ‘‘leftover’’ term at the right-hand side of Eq. (4), which does not depend on $\delta n_{\mathbf{r}}$, eventually provides the effective Hamiltonian describing the phase fluctuations of the $|\psi|^4$ model (that are the relevant, low-lying degrees of freedom close to the BKT phase transition [67]). Substituting each $\bar{n}_{\mathbf{r}}$ at the right-hand side of Eq. (4) with the corresponding saddle-point solution of Eq. (5), we conclude that the phase fluctuations are described by the modulated x - y Hamiltonian H_{x-y}^{mod} , given by

$$H_{x-y}^{\text{mod}} = -2 \sum_{\mathbf{r}} \{J_{\mathbf{r}}^x \cos[\theta_{(l_x+1, l_y)} - \theta_{(l_x, l_y)}] + J_{\mathbf{r}}^y \cos[\theta_{(l_x, l_y+1)} - \theta_{(l_x, l_y)}]\}, \quad (6)$$

with $J_{\mathbf{r}}^x = t\sqrt{\bar{n}_{(l_x, l_y)}\bar{n}_{(l_x+1, l_y)}}$ and $J_{\mathbf{r}}^y = t\sqrt{\bar{n}_{(l_x, l_y)}\bar{n}_{(l_x, l_y+1)}}$. Given the periodic form of the uniaxial modulation (2), we obtain that $J_{(l_x, l_y+N)}^{x(y)} = J_{(l_x, l_y)}^{x(y)}$, with $N = L/m$ being the modulation period. Moreover, since $\bar{n}_{(l_x, l_y)}$ is uniform along the x direction, (that is, it is independent of l_x , just as $\mu_{(l_x, l_y)}$), we infer that both J^x and J^y are functions of l_y only. Finally, as we evidenced above, $\bar{n}_{\mathbf{r}}$ is finite over every lattice site, which implies that $J_{\mathbf{r}}^x$ and $J_{\mathbf{r}}^y$ are different from 0 over every bond of the lattice.

Given the correspondence between H in Eq. (1) and H_{x-y}^{mod} , we refer to this latter model Hamiltonian to compute the superfluid fractions in the two directions as a function of the temperature T , $\rho_{s,x}(T)$ and $\rho_{s,y}(T)$. Specifically [8], we ‘‘twist’’ $\theta_{\mathbf{r}} \rightarrow \theta_{\mathbf{r}} + Q_x \frac{l_x}{L} + Q_y \frac{l_y}{L}$ and identify the superfluid fractions $\rho_{s,x}(T)$ and $\rho_{s,y}(T)$ from the coefficients of the quadratic (in Q_x and Q_y) contributions to the total free energy. In the low-temperature limit, we resort to an ‘‘improved’’ Villain approximation [8], i.e., we expand $\cos(\theta_{\mathbf{r}} - \theta_{\mathbf{r}'})$ up to fourth-order in $\theta_{\mathbf{r}} - \theta_{\mathbf{r}'}$. Expanding up to fourth-order allows us to recover the leading, low- T contributions to $\rho_{s,x(y)}(T)$ and $\rho_{s,x(y)}^{(0)}(T)$, without accounting for the contributions from vortex excitations, which we introduce later on, within the

renormalization group (RG) approach to the BKT phase transition.

In implementing the Villain approximation, one has to account suitably for the ‘‘superperiodicity’’ induced by the modulation. To do so, we write the Fourier mode expansion of $\theta_{(l_x, l_y)}$ and of $J_{l_y}^{x(y)}$ as

$$\theta_{(l_x, l_y)} = \frac{1}{L^2} \sum_{\mathbf{k} \in \mathcal{B}_N} \sum_{\nu=0}^{N-1} e^{i\mathbf{k} \cdot \mathbf{r} + \frac{2\pi i \nu l_y}{N}} \theta_{\mathbf{k}, \nu},$$

$$J_{l_y}^{x(y)} = \frac{1}{N} \sum_{\nu=0}^{N-1} e^{\frac{2\pi i \nu l_y}{N}} J^{x(y)}(\nu), \quad (7)$$

with the reduced Brillouin zone $\mathcal{B}_N = [-\pi, \pi] \times [-\frac{\pi}{N}, \frac{\pi}{N}]$. To recover the large-scale, low- \mathbf{k} effective description of our system, we systematically integrate over the $\theta_{\mathbf{k}, \nu}$ modes, with $\nu \neq 0$ so as to obtain an effective Hamiltonian only involving the $\nu = 0$ modes. In the Appendix we describe in detail the whole derivation. As a result, we eventually obtain

$$H_{\text{Eff, mod}}^{\text{Vil}}[\mathcal{Q}] = \frac{1}{2L^2} \sum_{\mathbf{k} \in \mathcal{B}_N} \Delta(\mathbf{k}) |\theta_{\mathbf{k}, 0}|^2 + \frac{[Q_x^2 \mathcal{J}^x(T) + Q_y^2 \mathcal{J}^y(T)]}{2N}. \quad (8)$$

In the Appendix we show that $\mathcal{J}^{x(y)}(T) = \mathcal{J}_0^{x(y)} - T \mathcal{J}_1^{x(y)}$ and we provide the explicit formulas for $\mathcal{J}_0^{x(y)}$ and for $\mathcal{J}_1^{x(y)}$. Therefore, from Eq. (8) we determine the (‘‘bare,’’ that is, undressed by vortices) superfluid fractions along the two directions, according to

$$\rho_{s,x}^{(0)}(T) = \frac{\mathcal{J}^x(T)}{\mathcal{J}^x(0)} = 1 - \frac{T}{\delta_x},$$

$$\rho_{s,y}^{(0)}(T) = \frac{\mathcal{J}^y(T)}{\mathcal{J}^y(0)} = 1 - \frac{T}{\delta_y}, \quad (9)$$

with $\delta_{x(y)} = \mathcal{J}_0^{x(y)}/\mathcal{J}_1^{x(y)}$. In Eq. (A7) we provide the explicit formula for the kernel $\Delta(\mathbf{k})$. By expanding $\Delta(\mathbf{k})$ up to second order in \mathbf{k} , we obtain

$$H_{\text{Eff, mod}}^{\text{Vil}} = H_{\text{Eff, mod}}^{\text{Vil}}[\mathcal{Q} = \mathbf{0}] \approx \frac{1}{2L^2} \sum_{\mathbf{k}} \{\mathcal{J}^x(T)k_x^2 + \mathcal{J}^y(T)k_y^2\} |\theta_{\mathbf{k}, 0}|^2. \quad (10)$$

The right-hand side of Eq. (10) corresponds to the long-wavelength expansion of the Hamiltonian of a uniform, anisotropic x - y model with coupling strengths in the two directions respectively given by $\mathcal{J}^x(T)$ and $\mathcal{J}^y(T)$. Therefore, in the following we employ this latter model to account for the effect of the vortices on the superfluid fractions.

The BKT superfluid transition. In the general framework of the x - y model it is well established that, on taking into account vortex excitations, the ‘‘renormalized’’ superfluid fractions $\rho_{s,x(y)}$ acquire an explicit dependence on the running scale λ (eventually identified with the system size) [7,8,68]. Denoting with $y(T, \lambda)$, with $\rho_x(T, \lambda)$, and with $\rho_y(T, \lambda)$, respectively, the scale-dependent single-vortex fugacity and the superfluid fractions, their scaling with λ is described by the (anisotropic)

RG equations given by [7,66,68]

$$\begin{aligned} \frac{dy(T, \lambda)}{d \ln \lambda} &= \left[2 - \frac{\pi \mathcal{J}}{T} \sqrt{\rho_{s,x}(T, \lambda) \rho_{s,y}(T, \lambda)} \right] y(T, \lambda), \\ \frac{d\rho_{s,x}(T, \lambda)}{d \ln \lambda} &= -\frac{2\pi^3 \mathcal{J}}{T} y^2(T, \lambda) \sqrt{[\rho_{s,x}(T, \lambda)]^3 \rho_{s,y}(T, \lambda)}, \\ \frac{d\rho_{s,y}(T, \lambda)}{d \ln \lambda} &= -\frac{2\pi^3 \mathcal{J}}{T} y^2(T, \lambda) \sqrt{[\rho_{s,y}(T, \lambda)]^3 \rho_{s,x}(T, \lambda)}, \end{aligned} \quad (11)$$

with $\mathcal{J} = \sqrt{\mathcal{J}^x(0)\mathcal{J}^y(0)}$. The superfluid fractions in the thermodynamic limit are recovered from the solutions of Eq. (11) at given λ and T , determined by using the bare superfluid fractions in Eq. (9) as initial values of the parameters at the reference scale, by eventually taking the $\lambda \rightarrow \infty$ limit. The single-vortex fugacity at the reference scale, $y^{(0)}(T)$, can be estimated using a pertinent extension to the anisotropic model of the results of Ref. [8], which is $y^{(0)}(T) \approx \exp[-\frac{\pi^2 \mathcal{J}}{2T}]$. Over a finite-size (L^2) lattice, we recover the finite-size superfluid fractions $\rho_{s,x(y)}(T, L)$ by stopping the RG flow determined by Eq. (11) at $\lambda = L$.

To solve Eq. (11), we note that they imply that the dimensionless quantity $\mathcal{K}(T) = \rho_{s,y}(T, \lambda)/\rho_{s,x}(T, \lambda)$ is constant along the RG trajectories; that is, it is independent of λ . Accordingly, we set

$$\begin{aligned} \rho_{s,x}(T, \lambda) &= \rho_s(T, \lambda) \sqrt{\mathcal{K}(T)}, \\ \rho_{s,y}(T, \lambda) &= \rho_s(T, \lambda) / \sqrt{\mathcal{K}(T)}. \end{aligned} \quad (12)$$

In terms of $y(T, \lambda)$ and $\rho_s(T, \lambda)$, the system (11) reduces to

$$\begin{aligned} \frac{dy(T, \lambda)}{d \ln \lambda} &= \left[2 - \frac{\pi \mathcal{J}}{T} \rho_s(T, \lambda) \right] y(T, \lambda), \\ \frac{d\rho_s(T, \lambda)}{d \ln \lambda} &= -\frac{2\pi^3 \mathcal{J}}{T} y^2(T, \lambda) \rho_s(T, \lambda)^2. \end{aligned} \quad (13)$$

Equations (13) correspond to the familiar set of the BKT RG equations for the running parameters in the isotropic $x-y$ model [68]. It is, therefore, immediate to infer they imply that the critical temperature T_c satisfies the equation [68]

$$2\pi y^{(0)}(T_c) + 2 - \frac{\pi \mathcal{J}}{T_c} \rho_s^{(0)}(T_c) = 0, \quad (14)$$

with $\rho_s^{(0)}(T) = \sqrt{\rho_{s,x}^{(0)}(T) \rho_{s,y}^{(0)}(T)}$. (Roughly speaking, Eq. (14) implies a scaling of T_c with \mathcal{J} , as it is typical of the anisotropic $x-y$ model [69]).

Finally, we recover the ‘‘anisotropic’’ universal jump condition for the superfluid fractions, consistent with $\mathcal{K}(T)$ being invariant along the RG trajectories, given by

$$\begin{aligned} \lim_{T \rightarrow T_c^-} \rho_{s,x}(T) &= \frac{2T_c}{\pi \mathcal{J} \sqrt{\mathcal{K}(T_c)}}, \\ \lim_{T \rightarrow T_c^+} \rho_{s,x}(T) &= 0, \end{aligned} \quad (15)$$

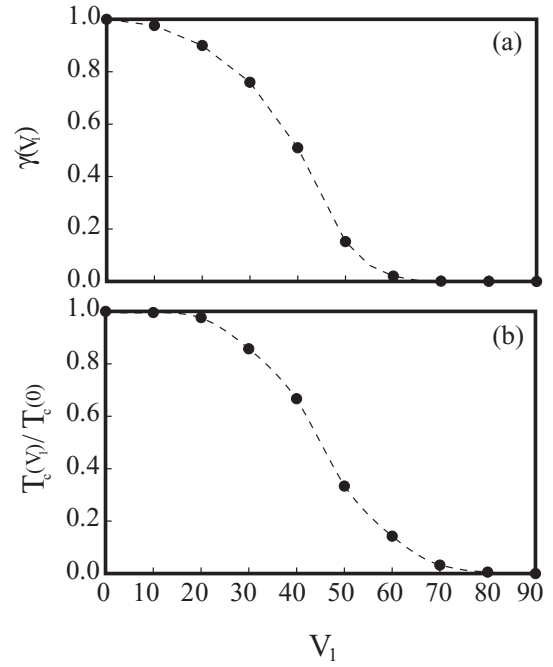


FIG. 1. (a) Effective anisotropy $\gamma(V_1) \equiv \mathcal{J}_y(0)/\mathcal{J}_x(0)$ induced in the equivalent $x-y$ Hamiltonian $H_{\text{Eff,mod}}^{\text{Vil}}$ by the external modulation. (b) Critical temperature for the BKT phase transition as a function of V_1 , $T_c(V_1)$, normalized to the critical temperature in the absence of modulation, $T_c(0)$. In both panels, the interpolating dashed line is a guide to the eye.

and

$$\begin{aligned} \lim_{T \rightarrow T_c^-} \rho_{s,y}(T) &= \frac{2T_c \sqrt{\mathcal{K}(T_c)}}{\pi \mathcal{J}}, \\ \lim_{T \rightarrow T_c^+} \rho_{s,y}(T) &= 0, \end{aligned} \quad (16)$$

with $\rho_{s,x(y)}(T) = \lim_{\lambda \rightarrow \infty} \rho_{s,x(y)}(T, \lambda)$.

For a finite system size L , Eq. (11) predict a downturn in both $\rho_{s,x}(T, L)$ and $\rho_{s,y}(T, L)$ as a function of T , centered over a certain ‘‘finite-size critical temperature’’ $T_c(L)$ (which is the same for both the superfluid fractions). The larger L is, the sharper the downturn in the superfluid fractions is. In the thermodynamic limit $L \rightarrow \infty$, the downturn evolves into the sharp ‘‘universal critical jump’’: the fingerprint of the BKT phase transition in a two-dimensional system [6–8].

The uniaxial modulation induces an effective anisotropy, as illustrated in Fig. 1(a), where the ratio $\gamma(V_1) \equiv \mathcal{J}_y(0)/\mathcal{J}_x(0)$, computed based on Eq. (A4) and (A6), is shown for the value of the model parameters used here (see above). There is a monotonic decrease, the system remaining two-dimensional for arbitrarily large values of V_1 . It is worth stressing that modulating the hopping rather than the potential [66] would possibly lead to a similar effective description of the scaling of the superfluid fractions.

Figure 1(b) also shows the computed critical temperature for the BKT phase transition as a function of V_1 , normalized to the critical temperature in the absence of modulation, $T_c(V_1)/T_c(0)$, as a function of V_1 . As one might intuitively expect, the quantities shown in Figs. 1(a) and 1(b) behave similarly as a function of V_1 . Indeed, in the limit $|V_1/V_0| \ll 1$,

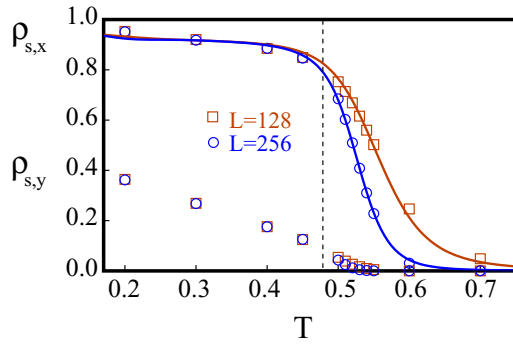


FIG. 2. Superfluid responses $\rho_{s,x}(T, L)$ and $\rho_{s,y}(T, L)$ of model (1), computed by means of the Monte Carlo approach as a function of T for $V_0 = U = 40$, $t = 1$, and modulation strength $V_1 = 40$, for different system sizes. The dashed vertical line marks the location of the transition, i.e., $T = T_c$. Also shown are fitting curves obtained as explained in the text.

a perturbative calculation based on the formalism of the Appendix shows that both quantities decrease quadratically with V_1 , while in the opposite limit the numerical results indicate a change of convexity; i.e., both quantities approach zero asymptotically.

IV. NUMERICAL RESULTS

In order to obtain an unbiased numerical check of our predictions, we performed Monte Carlo numerical simulations of the lattice field theory (1), specifically computing the superfluid responses $\rho_{s,x}(T, L)$ and $\rho_{s,y}(T, L)$ as a function of T for various system sizes. We used the classical worm algorithm, in its standard lattice implementation described, for instance, in Ref. [70]. In particular, the superfluid fraction is estimated by means of the well-known winding number estimator.

We henceforth take t as our energy unit and set $V_0 = U = 40$; i.e., we work in the strong-coupling limit of the theory, in which Eq. (1) approaches the isotropic x - y model in the absence of external modulation. For definiteness, but without any loss of generality, we set the period of the modulation of the external potential $N = 8$ lattice sites.

Figure 2 shows Monte Carlo results for $\rho_{s,x}(T, L)$ and $\rho_{s,y}(T, L)$, computed for two different system sizes, namely, $L = 128$ and $L = 256$, for a value of the amplitude of the modulating external potential $V_1 = 40$. The downturn in both $\rho_{s,x}(T, L)$ and $\rho_{s,y}(T, L)$ at a temperature of $T_c \approx 0.48$ is clear, although it is less evident in $\rho_{s,y}(T, L)$, due to the anisotropy-induced reduction of the superfluid fraction in the direction of the modulation [69]. As expected, the transition becomes increasingly sharp as L grows; despite the presence of the modulating field, the evidence of a BKT phase transition in the planar model seems clear. Obviously, however, this assertion must be verified by carrying out finite-size scaling analysis.

On integrating the RG equations (11) up to $\lambda = L$ for different values of T , one can obtain fitting curves for $\rho_{s,x}(T, L)$ and $\rho_{s,y}(T, L)$. To do this analytically, one needs to know how the system parameters at the reference scale depend on the

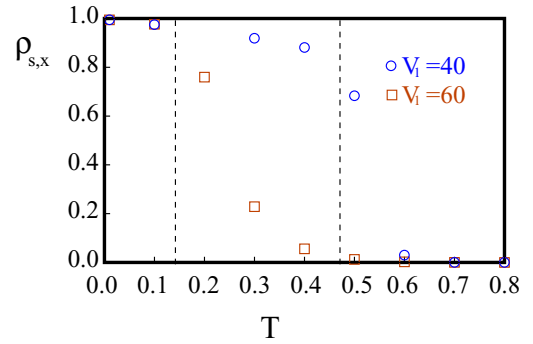


FIG. 3. Superfluid response $\rho_{s,x}(T, L)$ of the model (1) as a function of T , computed by Monte Carlo simulations for a square lattice with $L^2 = 256^2$ sites. The amplitudes of the modulation are $V_1 = 40$ (circles) and $V_1 = 60$ (squares), while the values of all other model parameters are specified in the text. The dashed vertical lines mark the approximate locations of the two critical temperatures.

temperature. Equations (9) and the expressions for δ_x and δ_y in the Appendix rely upon approximations that are strictly speaking only valid in the $T \rightarrow 0$ limit and thus are not expected to hold quantitatively near T_c . For this reason, we fitted the Monte Carlo results with the curves described in Sec. III, using δ_x , δ_y , and \mathcal{J} as adjustable fitting parameters. The excellent fit to the numerical data obtained in this way (shown in Fig. 2) represents strong evidence to the effect that the superfluid properties of model (1) are the same as those of the (anisotropic) x - y model [71].

Within the framework of the anisotropic x - y model, one expects a reduction of T_c with increasing anisotropy, consistent with Eq. (14). In Fig. 3, we show $\rho_{s,x}(T, L)$ as a function of T . The reduction of T_c on increasing V_1 (that is, the anisotropy in the effective x - y Hamiltonian) is apparent (in the figure we mark with dashed vertical lines the approximate locations of the two critical temperatures) and is also roughly consistent with the results for the anisotropy and for the critical temperature in Fig. 1 and with the implication of Eq. (14).

In our view, these results provide robust numerical confirmation of the theory described in Sec. III, namely, that the superfluid behavior of the $|\psi|^4$ theory in the presence of a uniaxial modulation reduces to that of the two-dimensional anisotropic x - y model. Accordingly, increasing the strength of the modulation simply enhances the anisotropy, thus pushing the BKT phase transition to lower values of T_c but without determining any dimensional crossover in the system. There is always a finite, though small, T_c at which the system undergoes the BKT phase transition from the superfluid to the disordered phase.

To strengthen our conclusion that T_c remains finite in the $V_1 \rightarrow \infty$ limit, in Fig. 4 we show our numerical results for $\rho_{s,x}(T, L)$ as a function of T for increasing values of L , from $L = 64$ till $L = 512$, for $t = 1$, $U = V_0 = 40$, and $V_1 = 40$ (a), and $V_1 = 60$ (b). In both cases we recognize the typical scaling of the superfluid fractions in the anisotropic x - y model, with T_c finite and consistent with the fitted data for T_c as a function of V_1 in Fig. 1.

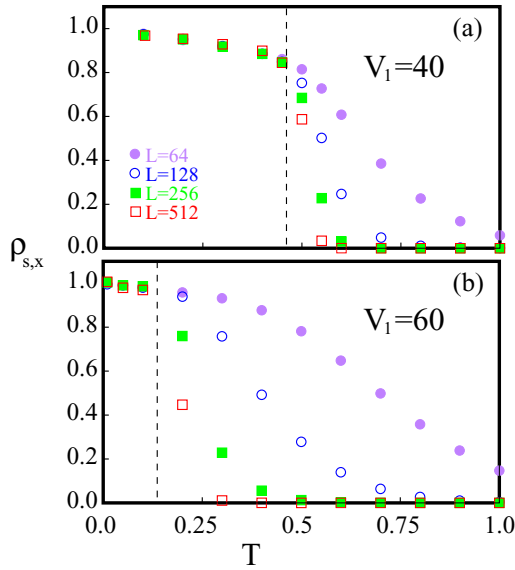


FIG. 4. Superfluid response $\rho_{s,x}(T, L)$ of the model (1) as a function of T , computed by Monte Carlo simulations for a square lattice for $L = 64$ (purple solid dots), $L = 128$ (blue empty dots), $L = 256$ (green solid squares), and $L = 512$ (red empty squares), and for $V_1 = 40$ (a) and $V_1 = 60$ (b). The dashed vertical lines mark the (approximate) location of the critical temperature in the two cases.

V. DISCUSSION AND CONCLUSIONS

In this paper, we investigated the effects of a uniaxial external modulation over a two-dimensional superfluid. We described the superfluid at finite temperature by means of the classical $|\psi|^4$ model over a square lattice. Adding the modulation on top of the well-established mapping between the $|\psi|^4$ model and the x - y model, we derived a version of the latter model Hamiltonian with modulated parameters, which allowed us to spell out the effects of progressively increasing the potential modulation strength V_1 .

We show that despite the tendency of the system to develop quasi-1D stripes perpendicular to the direction of the modulation, at any V_1 the superfluid phase transition is well captured by the classical anisotropic x - y model, to which the modulated model reduces in the long-wavelength, low-energy limit. In particular, the main effect of increasing V_1 is that of enhancing the anisotropy of the effective x - y Hamiltonian and, correspondingly, pushing T_c toward lower (though finite) values [72–74].

Due to the wide applicability of our minimal model to describing the superfluid phase transition in planar, interacting bosonic systems, we infer that, as a general result, an external uniaxial modulation fails to induce a 2D to 1D dimensional crossover in such a system. The good agreement between the analytical prediction and the numerical Monte Carlo data witnesses the reliability of our results, regardless of the various approximations we employed along our derivation. In addition, the finite-size scaling analysis of the superfluid fractions unambiguously shows that even for relatively large modulation amplitudes the scaling behavior is that expected for a 2D system, which is completely different from the 1D case [7,11,12,66,68,74].

Possible further extensions of our work include, but are not limited to, considering the inclusion of disorder in the sample. It would be interesting to evidence whether the scenario we evidenced is affected by impurities. In this direction, given the high level of control reached in the technology of cold-atom devices one may think, for instance, of engineering impurities “ad hoc,” with tunable parameters, mimicking junctions of quantum wires [75–81], or even network of junctions [82], with a high level of quantum coherence [83,84] and a plethora of potential practical applications.

ACKNOWLEDGMENTS

We thank Pasquale Sodano, Andrea Trombettoni, and Nikolay Prokof’ev for insightful discussions. A.N. and D.G. acknowledge financial support from Italy’s MIUR PRIN project TOP-SPIN (Grant No. PRIN 20177SL7HC). This work was also supported by the Natural Sciences and Engineering Research Council of Canada (NSERC). M.B. acknowledges the hospitality of the Università della Calabria, where part of this research work was carried out.

APPENDIX: DERIVATION OF EQ. (8)

In this Appendix we show that, once expressed in terms of the $\theta_{\mathbf{k},0}$, the Hamiltonian $H_{\text{Eff,mod}}^{\text{Vil}}[Q]$ takes the form in Eq. (8).

We begin with the mode expansions in Eq. (7). Denoting with $H_{x-y}^{\text{mod}}[Q]$ the Hamiltonian in Eq. (6) at nonzero Q , we approximate

$$H_{x-y}^{\text{mod}} \approx H_{\text{Vil},2}^{\text{mod}}[Q] + H_{\text{Vil},4}^{\text{mod}}[Q]. \quad (\text{A1})$$

The quadratic term in Eq. (A1) is given by

$$\begin{aligned} H_{\text{Vil},2}^{\text{mod}}[Q] = & \frac{1}{2NL^2} \sum_{v,v'=0}^{N-1} \sum_{\mathbf{k} \in \mathcal{B}_N} \theta_{-\mathbf{k},-v} \theta_{\mathbf{k},v'} \mathcal{D}_{v,v'}(\mathbf{k}) \\ & + \frac{[Q_x^2 J^x(0) + Q_y^2 J^y(0)]}{2N} \\ & + \frac{Q_y}{NL} \sum_{v=1}^{N-1} \theta_{0,v} (e^{\frac{2\pi i v}{N}} - 1) J^y(-v), \end{aligned} \quad (\text{A2})$$

with

$$\begin{aligned} \mathcal{D}_{v,v'}(\mathbf{k}) = & |1 - e^{i k_x}|^2 J_x(v - v') \\ & + (1 - e^{-i k_y - \frac{2\pi i v}{N}})(1 - e^{i k_y + \frac{2\pi i v'}{N}}) J_y(v - v'). \end{aligned} \quad (\text{A3})$$

As for the quartic term, we treat it within the mean-field approximation, along the derivation of Ref. [8]. This implies decoupling quartic and cubic terms, respectively, according to $\sum_{\mathbf{r}} J_y^x [\theta_{(l_x+1,l_y)} - \theta_{(l_x,l_y)}]^4 \rightarrow \sum_{\mathbf{r}} J_y^x [\theta_{(l_x+1,l_y)} - \theta_{(l_x,l_y)}]^2 \langle [\theta_{(l_x+1,l_y)} - \theta_{(l_x,l_y)}]^2 \rangle$, together with the analogous expression with $x \rightarrow y$, and to $\sum_{\mathbf{r}} J_y^y [\theta_{(l_x,l_y+1)} - \theta_{(l_x,l_y)}]^3 \rightarrow \sum_{\mathbf{r}} J_y^y [\theta_{(l_x,l_y+1)} - \theta_{(l_x,l_y+1)}] \langle [\theta_{(l_x,l_y+1)} - \theta_{(l_x,l_y)}]^2 \rangle$, with $\langle \dots \rangle$ denoting the average with respect to the quadratic Hamiltonian (A2). Just as for the homogeneous, isotropic Hamiltonian, the contributions obtained in this way simply amount to

adding finite- T corrections to $J^x(\nu)$ and $J^y(\nu)$, according to

$$\begin{aligned}
J^x(\nu) &\rightarrow \hat{J}^x(\nu, T) \\
&= J^x(\nu) - \frac{NT}{2} \sum_{\nu_1, \nu_2=0}^{N-1} J^x(\nu + \nu_1 - \nu_2) \\
&\quad \times \frac{1}{L^2} \sum_{\mathbf{q} \in \mathcal{B}_N} |1 - e^{iq_x}|^2 [\mathcal{D}(\mathbf{q})]_{\nu_1, \nu_2}^{-1}, \\
J^y(\nu) &\rightarrow \hat{J}^y(\nu, T) \\
&= J^y(\nu) - \frac{NT}{2} \sum_{\nu_1, \nu_2=0}^{N-1} J^y(\nu + \nu_1 - \nu_2) \\
&\quad \times \frac{1}{L^2} \sum_{\mathbf{q} \in \mathcal{B}_N} (1 - e^{-iq_y - \frac{2\pi i \nu_1}{N}}) \\
&\quad \times (1 - e^{iq_y + \frac{2\pi i \nu_2}{N}}) [\mathcal{D}(\mathbf{q})]_{\nu_1, \nu_2}^{-1}. \tag{A4}
\end{aligned}$$

Once the $\theta_{\mathbf{k}, \nu}$ modes are pertinently integrated over, the free energy of our system must be quadratic in the $\mathcal{Q}_{x,y}$. To evidence this, we trade $\hat{H}_{\text{Vil},2}^{\text{mod}}[\mathcal{Q}]$ [that is, $H_{\text{Vil},2}^{\text{mod}}[\mathcal{Q}]$ with all $J^{x(y)}(\nu)$ substituted with $\hat{J}^{x(y)}(\nu, T)$] for the effective Villain Hamiltonian $H_{\text{Eff},\text{mod}}^{\text{Vil}}[\mathcal{Q}]$, defined (apart for an unessential constant) via a systematic integration over the $\theta_{\mathbf{k}, \nu}$ modes,

with $\nu \neq 0$, according to

$$e^{-\frac{H_{\text{Eff},\text{mod}}^{\text{Vil}}[\mathcal{Q}]}{T}} = \int \prod_{\mathbf{k}} \prod_{\nu=1}^{N-1} d\theta_{\mathbf{k}, \nu} e^{-\frac{\hat{H}_{\text{Vil},2}^{\text{mod}}[\mathcal{Q}]}{T}}. \tag{A5}$$

As a result, we obtain Eq. (8) of the main text, with

$$\begin{aligned}
\mathcal{J}^x(T) &= \hat{\mathcal{J}}^x(0, T) \equiv \mathcal{J}_0^x - T \mathcal{J}_1^x, \\
\mathcal{J}^y(T) &= \hat{\mathcal{J}}^y(0, T) - \sum_{\nu_1, \nu_2=1}^{N-1} \hat{\mathcal{J}}^y(\nu_1, T) (1 - e^{-\frac{2\pi i \nu_1}{N}}) \\
&\quad \times [\tilde{\mathcal{D}}(\mathbf{0})]_{\nu_1, \nu_2}^{-1} (1 - e^{\frac{2\pi i \nu_2}{N}}) \hat{\mathcal{J}}^y(-\nu_2, T) \\
&\equiv \mathcal{J}_0^y - T \mathcal{J}_1^y. \tag{A6}
\end{aligned}$$

Setting $\delta_{x(y)} = \mathcal{J}_0^{x(y)} / \mathcal{J}_1^{x(y)}$ yields Eq. (9) of the main text. The kernel $\Delta(\mathbf{k})$ in Eq. (8) is defined as

$$\Delta(\mathbf{k}) = \hat{\mathcal{D}}_{0,0}(\mathbf{k}) - \sum_{\nu, \nu'=1}^{N-1} \hat{\mathcal{D}}_{0,\nu}(\mathbf{k}) [\tilde{\mathcal{D}}^{-1}(\mathbf{k})]_{\nu, \nu'} \hat{\mathcal{D}}_{\nu',0}(\mathbf{k}), \tag{A7}$$

with $\tilde{\mathcal{D}}(\mathbf{k})$ in Eq. (A6) being an $(N-1) \times (N-1)$ matrix, obtained from $\hat{\mathcal{D}}(\mathbf{k})$ by dropping the first row and the first column, with $\hat{\mathcal{D}}_{\nu, \nu'}(\mathbf{k})$ equal to $\mathcal{D}_{\nu, \nu'}(\mathbf{k})$ in Eq. (A3), and with $J^{x(y)}(\nu)$ substituted with $\hat{J}^{x(y)}(\nu, T)$. Expanding $\Delta(\mathbf{k})$ around $\mathbf{k} = \mathbf{0}$ up to second order in \mathbf{k} , we obtain Eq. (10) of the main text.

-
- [1] A. J. Leggett, *Quantum Liquids: Bose Condensation and Cooper Pairing in Condensed-Matter Systems* (Oxford University, Oxford, England, 2006).
- [2] Y. Kora, M. Boninsegni, D. T. Son, and S. Zhang, *Proc. Natl. Acad. Sci. USA* **117**, 27231 (2020).
- [3] V. L. Berezinskii, *Sov. Phys. JETP* **34**, 610 (1972).
- [4] J. M. Kosterlitz and D. J. Thouless, *J. Phys. C: Solid State Phys.* **5**, L124 (1972).
- [5] J. M. Kosterlitz and D. J. Thouless, *J. Phys. C: Solid State Phys.* **6**, 1181 (1973).
- [6] D. R. Nelson and J. M. Kosterlitz, *Phys. Rev. Lett.* **39**, 1201 (1977).
- [7] J. V. José, L. P. Kadanoff, S. Kirkpatrick, and D. R. Nelson, *Phys. Rev. B* **16**, 1217 (1977).
- [8] T. Ohta and D. Jasnow, *Phys. Rev. B* **20**, 139 (1979).
- [9] H. Weber and P. Minnhagen, *Phys. Rev. B* **37**, 5986 (1988).
- [10] F. D. M. Haldane, *Phys. Rev. Lett.* **47**, 1840 (1981).
- [11] A. Del Maestro and I. Affleck, *Phys. Rev. B* **82**, 060515(R) (2010).
- [12] A. Del Maestro, M. Boninsegni, and I. Affleck, *Phys. Rev. Lett.* **106**, 105303 (2011).
- [13] W. A. Little, *Phys. Rev.* **156**, 396 (1967).
- [14] J. S. Langer and V. Ambegaokar, *Phys. Rev.* **164**, 498 (1967).
- [15] D. E. McCumber and B. I. Halperin, *Phys. Rev. B* **1**, 1054 (1970).
- [16] A. D. Zaikin, D. S. Golubev, A. van Otterlo, and G. T. Zimányi, *Phys. Rev. Lett.* **78**, 1552 (1997).
- [17] J. A. Freire, D. P. Arovas, and H. Levine, *Phys. Rev. Lett.* **79**, 5054 (1997).
- [18] Y. Kagan, N. V. Prokof'ev, and B. V. Svistunov, *Phys. Rev. A* **61**, 045601 (2000).
- [19] S. I. Shevchenko, *Sov. J. Low Temp. Phys.* **14**, 553 (1988).
- [20] M. Boninsegni, A. B. Kuklov, L. Pollet, N. V. Prokof'ev, B. V. Svistunov, and M. Troyer, *Phys. Rev. Lett.* **99**, 035301 (2007).
- [21] D. J. Bishop and J. D. Reppy, *Phys. Rev. Lett.* **40**, 1727 (1978).
- [22] G. Agnolet, D. F. McQueeney, and J. D. Reppy, *Phys. Rev. B* **39**, 8934 (1989).
- [23] G. A. Csáthy, D. Tulimieri, J. Yoon, and M. H. W. Chan, *Phys. Rev. Lett.* **80**, 4482 (1998).
- [24] M. Boninsegni, M. W. Cole, and F. Toigo, *Phys. Rev. Lett.* **83**, 2002 (1999).
- [25] E. Van Cleve, P. Taborek, and J. E. Rutledge, *J. Low Temp. Phys.* **150**, 1 (2008).
- [26] J. M. Kosterlitz, *J. Low Temp. Phys.* **201**, 541 (2020).
- [27] K. Epstein, A. M. Goldman, and A. M. Kadin, *Phys. Rev. Lett.* **47**, 534 (1981).
- [28] D. J. Resnick, J. C. Garland, J. T. Boyd, S. Shoemaker, and R. S. Newrock, *Phys. Rev. Lett.* **47**, 1542 (1981).
- [29] Z. Hadzibabic, P. Krüger, M. Cheneau, B. Battelier, and J. Dalibard, *Nature (London)* **441**, 1118 (2006).
- [30] R. Desbuquois, L. Chomaz, T. Yefsah, J. Léonard, J. Beugnon, C. Weitenberg, and J. Dalibard, *Nat. Phys.* **8**, 645 (2012).
- [31] R. J. Fletcher, M. Robert-de-Saint-Vincent, J. Man, N. Navon, R. P. Smith, K. G. H. Viebahn, and Z. Hadzibabic, *Phys. Rev. Lett.* **114**, 255302 (2015).
- [32] S. Sunami, V. P. Singh, D. Garrick, A. Beregi, A. J. Barker, K. Luksch, E. Bentine, L. Mathey, and C. J. Foot, *Phys. Rev. Lett.* **128**, 250402 (2022).

- [33] P. E. Sokol, M. R. Gibbs, W. G. Stirling, R. T. Azuah, and M. A. Adams, *Nature (London)* **379**, 616 (1996).
- [34] R. M. Dimeo, P. E. Sokol, C. R. Anderson, W. G. Stirling, K. H. Andersen, and M. A. Adams, *Phys. Rev. Lett.* **81**, 5860 (1998).
- [35] O. Plantevin, B. Fåk, H. R. Glyde, N. Mulders, J. Bossy, G. Coddens, and H. Schober, *Phys. Rev. B* **63**, 224508 (2001).
- [36] C. R. Anderson, K. H. Andersen, W. G. Stirling, P. E. Sokol, and R. M. Dimeo, *Phys. Rev. B* **65**, 174509 (2002).
- [37] R. Toda, M. Hieda, T. Matsushita, N. Wada, J. Taniguchi, H. Ikegami, S. Inagaki, and Y. Fukushima, *Phys. Rev. Lett.* **99**, 255301 (2007).
- [38] T. R. Prisk, N. C. Das, S. O. Diallo, G. Ehlers, A. A. Podlesnyak, N. Wada, S. Inagaki, and P. E. Sokol, *Phys. Rev. B* **88**, 014521 (2013).
- [39] M. Savard, G. Dauphinais, and G. Gervais, *Phys. Rev. Lett.* **107**, 254501 (2011).
- [40] W. Teizer, R. B. Hallock, E. Dujardin, and T. W. Ebbesen, *Phys. Rev. Lett.* **82**, 5305 (1999).
- [41] T. Ohba, *Sci. Rep.* **6**, 28992 (2016).
- [42] C. Blumenstein, J. Schaefer, S. Mietke, S. Meyer, A. Dollinger, M. Lochner, X. Y. Cui, L. Patthey, R. Matzdorf, and R. Claessen, *Nat. Phys.* **7**, 776 (2011).
- [43] T. Kinoshita, T. Wenger, and D. S. Weiss, *Science* **305**, 1125 (2004).
- [44] B. Yang, Y.-Y. Chen, Y.-G. Zheng, H. Sun, H.-N. Dai, X.-W. Guan, Z.-S. Yuan, and J.-W. Pan, *Phys. Rev. Lett.* **119**, 165701 (2017).
- [45] K. Cedergren, R. Ackroyd, S. Kafanov, N. Vogt, A. Shnirman, and T. Duty, *Phys. Rev. Lett.* **119**, 167701 (2017).
- [46] S. Lammers, I. Boettcher, and C. Wetterich, *Phys. Rev. A* **93**, 063631 (2016).
- [47] M. Wenzel, F. Böttcher, T. Langen, I. Ferrier-Barbut, and T. Pfau, *Phys. Rev. A* **96**, 053630 (2017).
- [48] G. Biagioni, N. Antolini, A. Alaña, M. Modugno, A. Fioretti, C. Gabbanini, L. Tanzi, and G. Modugno, *Phys. Rev. X* **12**, 021019 (2022).
- [49] M. Boninsegni, *J. Low Temp. Phys.* **168**, 137 (2012).
- [50] Y. Kora and M. Boninsegni, *J. Low Temp. Phys.* **197**, 337 (2019).
- [51] F. Meinert, M. Panfil, M. J. Mark, K. Lauber, J.-S. Caux, and H.-C. Nägerl, *Phys. Rev. Lett.* **115**, 085301 (2015).
- [52] G. Boéris, L. Gori, M. D. Hoogerland, A. Kumar, E. Lucioni, L. Tanzi, M. Inguscio, T. Giamarchi, C. D'Errico, G. Carleo, G. Modugno, and L. Sanchez-Palencia, *Phys. Rev. A* **93**, 011601(R) (2016).
- [53] H. Moraal, *Phys. A (Amsterdam, Neth.)* **85**, 457 (1976).
- [54] M. W. Cole, V. H. Crespi, G. Stan, C. Ebner, J. M. Hartman, S. Moroni, and M. Boninsegni, *Phys. Rev. Lett.* **84**, 3883 (2000).
- [55] M. Boninsegni, S.-Y. Lee, and V. H. Crespi, *Phys. Rev. Lett.* **86**, 3360 (2001).
- [56] T. Giamarchi, *Chem. Rev.* **104**, 5037 (2004).
- [57] P. Kalinay, *Eur. Phys. J.: Spec. Top.* **223**, 3027 (2014).
- [58] B. Béri and N. R. Cooper, *Phys. Rev. Lett.* **109**, 156803 (2012).
- [59] B. Béri, *Phys. Rev. Lett.* **110**, 216803 (2013).
- [60] A. Altland and R. Egger, *Phys. Rev. Lett.* **110**, 196401 (2013).
- [61] D. Giuliano, L. Lepori, and A. Nava, *Phys. Rev. B* **101**, 195140 (2020).
- [62] D. Giuliano, A. Nava, and P. Sodano, *Nucl. Phys. B* **960**, 115192 (2020).
- [63] D. Giuliano, A. Nava, R. Egger, P. Sodano, and F. Buccheri, *Phys. Rev. B* **105**, 035419 (2022).
- [64] F. Buccheri, A. Nava, R. Egger, P. Sodano, and D. Giuliano, *Phys. Rev. B* **105**, L081403 (2022).
- [65] M. E. Fisher, M. N. Barber, and D. Jasnow, *Phys. Rev. A* **8**, 1111 (1973).
- [66] J.-S. You, H. Lee, S. Fang, M. A. Cazalilla, and D.-W. Wang, *Phys. Rev. A* **86**, 043612 (2012).
- [67] M. Wallin, E. S. Sörensen, S. M. Girvin, and A. P. Young, *Phys. Rev. B* **49**, 12115 (1994).
- [68] C. Itzykson and J.-M. Drouffe, *Statistical Field Theory*, Cambridge Monographs on Mathematical Physics, Vol. 1 (Cambridge University, Cambridge, England, 1989).
- [69] G. A. Williams, *Phys. Rev. B* **73**, 214531 (2006).
- [70] N. Prokof'ev and B. Svistunov, *Phys. Rev. Lett.* **87**, 160601 (2001).
- [71] Similar plots can be drawn for $\rho_{s,y}$ as well, but the fitting procedure is rendered complicated by the small values of $\rho_{s,y}$ around T_c , making the agreement with numerical data less impressive than that for the x part.
- [72] K. Yamashita and D. S. Hirashima, *Phys. Rev. B* **79**, 014501 (2009).
- [73] W. Yang and I. Affleck, *Phys. Rev. B* **102**, 205426 (2020).
- [74] A. Nava, D. Giuliano, P. H. Nguyen, and M. Boninsegni, *Phys. Rev. B* **105**, 085402 (2022).
- [75] C. Chamon, M. Oshikawa, and I. Affleck, *Phys. Rev. Lett.* **91**, 206403 (2003).
- [76] M. Oshikawa, C. Chamon, and I. Affleck, *J. Stat. Mech.: Theory Exp.* **2006**, P02008 (2006).
- [77] C.-Y. Hou, A. Rahmani, A. E. Feiguin, and C. Chamon, *Phys. Rev. B* **86**, 075451 (2012).
- [78] D. Giuliano and P. Sodano, *Nucl. Phys. B* **770**, 332 (2007).
- [79] D. Giuliano and I. Affleck, *Nucl. Phys. B* **944**, 114645 (2019).
- [80] C. L. Kane, D. Giuliano, and I. Affleck, *Phys. Rev. Res.* **2**, 023243 (2020).
- [81] D. Guerci and A. Nava, *Phys. E (Amsterdam, Neth.)* **134**, 114895 (2021).
- [82] J. Medina, D. Green, and C. Chamon, *Phys. Rev. B* **87**, 045128 (2013).
- [83] E. Novais, A. H. Castro Neto, L. Borda, I. Affleck, and G. Zarand, *Phys. Rev. B* **72**, 014417 (2005).
- [84] D. Giuliano and P. Sodano, *New J. Phys.* **10**, 093023 (2008).